Results in Engineering 25 (2025) 104166

Contents lists available at ScienceDirect

Results in Engineering

journal homepage: www.sciencedirect.com/journal/results-in-engineering

Enhanced fault detection in zig-zag transformers: Insights from dissolved gas analysis and transient current analysis

Ricardo Manuel Arias Velásquez [a,*], Renato Fabricio Arias Velásquez [b]

[a] *Universidad Tecnológica del Perú, Peru*
[b] *Universidad Autónoma del Perú, Peru*

A R T I C L E I N F O

Keywords:
DGA
Oil
Transformer
Zig-zag

A B S T R A C T

This research article investigates the performance and fault detection capabilities of 35 zig-zag transformers connected to solar power plants in the medium voltage busbar, focusing on "dissolved gas analysis" (DGA) and fault diagnostics. Despite the absence of sudden disconnections, the transformers exhibited evolving failure modes. The study details the protection mechanisms employed, including overcurrent, overvoltage, and mechanical protections, integrated with a master trip system. Revealing significant deviations from normal levels before faults. Elevated hydrogen and methane levels, along with increased acetylene concentrations, indicated severe arcing and overheating, while treated oil samples showed a notable reduction in gas concentrations, underscoring the effectiveness of oil treatment in managing thermal and electrical stresses. This paper highlights the evolution of fault modes, including partial discharges, thermal faults, and arc faults, with specific diagnostic markers for each. The analysis of transient currents during faults indicated internal short circuits, leading to substantial mechanical and thermal damage, including core misalignment and tank deformation. The efficiency increases from 85.71 % in the detection with DGA to 91.43 % based on the combined analysis for DGA, comtrade and overcurrent analysis in the complete fleet.

1. Introduction

The growing penetration of renewable energy sources into the power grid necessitates advanced designs and robust technologies to ensure stability, efficiency, and reliability. In this context, zig-zag transformers, also known as interconnected-star transformers, play a pivotal role in addressing key challenges in renewable energy substations, such as grounding, harmonic suppression, and phase balancing.

Grounding is critical in three-phase electrical systems to minimize the potential difference between live terminals and the ground. While star (wye) configurations naturally provide a neutral for grounding, transformer substations with delta connections lack this feature. In such cases, grounding transformers, including zig-zag and wye-delta types, are employed to create a virtual neutral point. The zig-zag transformer, which has no secondary winding, connects its primary winding terminals to the system needing grounding. It presents low impedance to zero-sequence currents during ground faults, ensuring effective fault current management. For instance, when varying the ground path resistance, fault current characteristics change significantly. Without resistance, the RMS current can reach 600 A (peak 790 A). Adding a 5 Ω resistance reduces the RMS current to 580 A (peak 780 A), while a 20 Ω resistance decreases it further to 510 A (peak 670 A), and a 50 Ω resistance lowers it to 343 A (peak 451 A) [1].

In renewable energy substations, where power quality and stability are paramount, zig-zag transformers also provide a pathway for zero-sequence currents, enabling effective grounding. This is particularly crucial in scenarios where traditional grounding methods may be insufficient due to the variable and unpredictable nature of renewable energy generation. Studies indicate that residual voltage (V_o) downstream decreases by up to 30 % with the use of zig-zag transformers. However, upstream events during open-phase intervals show a 435 % increase in zero-sequence current ($3I_o$) and a 98 % increase in residual voltage, highlighting the high impedance fault results [2].

Additionally, zig-zag transformers contribute to harmonic suppression, which is essential in systems with renewable energy sources such as solar and wind. These sources often introduce harmonics that can degrade power quality, leading to issues such as overheating of equipment and malfunctioning of protective devices. The zig-zag transformer's design inherently mitigates harmonics, thereby enhancing system efficiency and reliability.

* Corresponding author.
E-mail address: ricardoariasvelasquez@hotmail.com (R.M. Arias Velásquez).

https://doi.org/10.1016/j.rineng.2025.104166
Received 19 July 2024; Received in revised form 1 January 2025; Accepted 23 January 2025
Available online 24 January 2025

The balancing properties of zig-zag transformers are particularly valuable in renewable energy applications, where intermittent and variable generation can cause unbalanced loads. By effectively balancing these loads, zig-zag transformers help maintain system performance within safe and optimal parameters, ensuring operational integrity [3].

Testing and simulation results further underscore the importance of optimizing design parameters for zig-zag transformers. For example, tests conducted with zero-sequence impedance values of 54 Ω/phase, 108 Ω/phase, and 216 Ω/phase yielded consistent results in both physical experiments and simulations. These findings emphasize the necessity of selecting appropriate grounding resistances and zero-sequence impedance values to maximize the performance and reliability of zig-zag transformers in renewable energy applications.

In addition to their grounding capabilities, wye-delta transformers also provide a low-impedance path for zero-sequence currents. Their primary neutral is connected to the ground, while the secondary delta winding can remain open or connect to a three-phase supply system. Both zig-zag and wye-delta transformers are integral to power system grounding, as detailed in standards like British Standard BS 7671:2000, which outlines grounding guidelines for low-voltage installations [4].

In conclusion, the design and implementation of zig-zag transformers in delta connections are vital for addressing grounding, harmonic, and phase-balancing challenges in renewable energy substations. These transformers improve power quality and system stability, facilitating the efficient integration of renewable energy sources into the grid. As the demand for renewable energy continues to grow, zig-zag transformers will play an increasingly critical role in ensuring a resilient and sustainable power infrastructure

1.1. Motivation

The increasing integration of renewable energy sources, particularly large-scale photovoltaic (PV) solar plants, into power grids has introduced significant challenges in managing short-circuit conditions. Conventional power systems rely on high-inertia synchronous generators, which provide substantial short-circuit currents during faults, ensuring the reliable operation of grid protection mechanisms. In contrast, renewable energy systems often utilize inverters with low inertia, resulting in much lower short-circuit currents. This disparity presents a critical challenge in maintaining grid stability and ensuring the effective operation of protection systems.

A deeper understanding of the implications of these low short-circuit currents is essential for the seamless integration of renewable energy sources into modern power grids. This research focuses on addressing these challenges, emphasizing the detection of internal faults in zig-zag transformers. These transformers face increased complexity in fault detection due to the inherently low short-circuit currents associated with renewable energy systems.

Furthermore, in power systems where the neutral point is unavailable—such as transformers connected in delta or those without accessible neutrals—an artificial neutral is often established using earthing transformers. In these configurations, the three line terminals are connected to a zig-zag transformer without a secondary winding. Each limb of the transformer contains two identical windings wound in opposite directions, which carry currents in differential mode. This study aims to investigate these critical aspects, providing insights and solutions that enhance the reliability and stability of power grids as they incorporate increasing shares of renewable energy.

1.2. Problem statement

The reliability of ground fault protection systems in medium-voltage solar plants is a critical concern, particularly when zig-zag transformers are employed for grounding. These systems are typically low-impedance grounded and demand precise protection settings to ensure fault selectivity and prevent unnecessary tripping during normal operations. However, a significant challenge lies in detecting internal faults within zig-zag transformers, which often remain undetected due to the limitations of traditional protection methods, such as overcurrent and zero-sequence voltage monitoring.

This challenge is exacerbated by the complex nature of fault evolution. Early indicators, such as stray gassing and partial discharge, can escalate into more severe conditions, including arc faults. Effective fault detection and isolation require methodologies tailored to the specific characteristics of zig-zag transformers, considering their unique operational conditions and fault behaviors. Additionally, the validation of protection settings, through both field data from 35 zig-zag transformers and laboratory analysis, reveals significant variations in gas concentrations indicative of different fault types. Current practices lack the ability to efficiently predict and prevent these faults, leading to potential catastrophic failures. This research aims to address the gaps in current fault detection methodologies by optimizing ground fault protection settings and enhancing the detection of internal faults in zig-zag transformers. By integrating dissolved gas analysis (DGA), Comtrade analysis, and overcurrent protection, the study seeks to improve fault recognition efficiency and reduce the risk of undetected faults that could compromise the safety and reliability of solar energy systems.

The paper includes the following sections: Section 2; it included the methodology for the detection of ground overcurrent for internal and external fault, and data description for 35 zig-zag transformers with application in solar technology, connected in the medium voltage bus bar of 30 to 36 kV, besides, the efficiency metrics. Section 3 develops the case study with sudden disconnection and failures modes in evolution.

2. Literature, methodology and data

2.1. Literature evaluation

Grounding faults in electrical systems necessitate effective neutral grounding techniques to maintain system stability and minimize damage. Earthing transformers, such as zig-zag transformers, are deployed to create an artificial neutral in delta-connected systems or when the neutral is unavailable. These transformers minimize flux and provide a stable neutral point for fault conditions. Several grounding methods, such as solid grounding, resistance grounding, and reactance grounding, are employed to manage fault currents effectively. Solid grounding neutralizes capacitive fault currents and prevents arcing grounds, while resistance grounding limits fault current magnitude using non-inductive resistors. Furthermore, its structure, comprising windings connected in a zig-zag pattern, effectively cancels out phase imbalances and ensures the proper redistribution of fault currents. This makes it particularly useful in mitigating fault currents in high-resistance grounding systems. However, the zig-zag transformer has inherent limitations. Leakage impedances within the transformer can cause a phase shift in the neutral point voltage, reducing its compensation accuracy and potentially hindering fault voltage suppression [18]. Reactance grounding employs adjustable reactors to resonate with system capacitances, achieving near-complete fault current compensation. Effective grounding, as defined by IEEE standards, ensures voltage rise in healthy phases does not exceed 80 % of line voltage, optimizing safety and reliability. For advanced applications, Gas-Insulated Substations (GISs) offer compact, high-reliability solutions using SF_6 gas for insulation and arc quenching. GIS substations require only 10 % of the space of conventional designs, making them ideal for urban or space-constrained areas, with enhanced resistance to environmental pollution and reduced installation costs. Such grounding and substation innovations underline the importance of tailored solutions in modern power systems [17].

About the modelling, its design ensures zero-sequence flux cancellation through phase windings arranged on two magnetic columns, resulting in a low zero-sequence impedance of <10 Ω and minimal no-load losses. This enables its operation at over 90 % of its power rating, making it a robust choice for grounding in traditional applications, in the generation regarding the wind parks and photovoltaic solar plants. In 2018, [19] incorporated symmetrical grounding windings in a delta-connected secondary, distributing the neutral current across three windings under unbalanced load conditions. This configuration provides stable three-phase voltages (220 V phase-to-ground and 380 V phase-to-phase) and additional mid-tap connections delivering 110 V for smaller loads. The multi-voltage capability simplifies microgrid network design, for ultra generation by using solar panels, as seen in applications in Taiwan. To enhance the analysis and optimization of such systems, a steady-state mathematical model, implemented in MATLAB/Simulink, has been developed. Therefore, in [19] validated through field tests, serves as a critical tool for the planning and operational design of distribution systems and microgrid networks; therefore, its winding configuration effectively suppresses harmonic currents and balances the system during unbalanced loads, in the Table 1.

In the context of the simulation, the zigzag transformer performs comparably to neutral grounding in terms of voltage and current stability, as evidenced by the minimal percentage differences in the magnitude of voltages (maximum error: −1.2207 %, equivalent to −0.102 V) and currents (maximum error: −0.9272 %, equivalent to −0.0013 A).

These results confirm its reliability in ensuring system stability under both balanced and unbalanced load conditions. In the renewable field, for instance for Taiwan, the transformer exhibits limitations under certain conditions, such as a slightly higher voltage error under no-load conditions (maximum error: 2.3226 %, equivalent to 0.214 V) and higher current error under unbalanced loads (maximum error: 4.8866 %, equivalent to 0.0237 A) [19].

About the application of zig-zag transformers in solar power plants, the configuration of the connection created high zero-sequence impedance while blocking positive and negative sequence components, except for minor leakage flux effects. Unlike delta-Y transformers, the zigzag transformer lacks galvanic isolation, functioning instead as a high-impedance reactor. Its advantages include lower material requirements, as it only needs to be rated for one-third of the grid-forming nominal power under severe unbalance conditions, making it a cost-effective solution. However, limitations include the inability to block zero-sequence harmonics entirely, as well as potential efficiency losses due to leakage fluxes. In quantitative terms, the zigzag transformer reduces stress on the main system components during unbalanced load conditions, ensuring smoother fault-tolerant operation when integrated with the proposed fault-tolerant converter topology. These attributes make it particularly suitable for microgrids, where robust handling of unbalanced conditions and efficient utilization of resources are essential.

Table 1
Trends and limitations.

Reference	Contribution	KPI	Limitation
[2]	Highlighted the decrease in residual voltage (V0) downstream by up to 30 %, and analyzed over 90 % of events showing increased residual voltage and current upstream during open phase intervals.	Residual voltage (V0) decreased by 30 %; 3I0 increased by 435 % during open phase; 98 % increase during other events.	High impedance faults pose challenges; no comprehensive fault detection under diverse operational conditions.
[4]	Discussed grounding methods using zig-zag and wye-delta transformers, focusing on providing stable grounding and minimizing fault currents.	Compliance with IEEE and BS 7671:2000 standards; low impedance path for zero-sequence currents.	Leakage impedances in zig-zag transformers can cause phase shifts, reducing compensation accuracy; wye-delta configurations lack harmonics suppression.
[17]	Evaluated advanced grounding techniques, including Gas-Insulated Substations (GISs), for urban and space-constrained environments.	Ground fault current reduction; compact design; reduced installation costs.	GIS systems require high initial investments; SF_6 gas usage raises environmental concerns.
[18]	Assessed zero-sequence flux cancellation and its role in fault mitigation in zig-zag transformers.	Low zero-sequence impedance (<10 Ω); operation at over 90 % power rating under balanced loads.	Slightly higher errors under no-load and unbalanced load conditions; higher voltage and current errors during unbalanced loads.
[19]	Developed and validated a MATLAB/Simulink model for analyzing zig-zag transformer performance in renewable energy systems.	Minimal voltage and current deviations under both balanced and unbalanced loads; efficient suppression of harmonics.	Higher current error under unbalanced loads (4.89 %); increased voltage error under no-load conditions (2.32 %).

2.2. Methodology

In the Fig. 1, describes the fault detection methodology for the zig-zag transformers, in this case, the ground fault overcurrent protection methodology employs a systematic process to ensure fault detection and enhance system stability and reliability. The process begins with monitoring the residual sum of three-phase currents under normal operating conditions, establishing a baseline for negligible residual current. When abnormalities arise, the grounding configuration is identified, including options such as zig-zag transformers with or without low-ohmic resistors or direct low-ohmic resistors to the transformer neutral. Protection settings are configured based on these configurations, with thresholds defined for overload protection (0.1 × In with an IEC Normal Inverse time delay) and short-circuit faults (50 % of fault current with a 100 ms delay). Fault detection involves continuous monitoring, differential current analysis, dissolved gas analysis (DGA), and post-fault evaluations. Additionally, selectivity configurations address cable susceptibility and long cable installations using directional neutral overcurrent protection (67 N). Efficiency is maximized through a combined methodology integrating DGA, Comtrade analysis, and differential protection, achieving superior fault detection and management.

Ground fault overcurrent protection operates by monitoring the residual sum of the three-phase currents. Under normal operating conditions, this residual sum is negligible, resulting in no significant current being measured. This characteristic enables the ground fault protection settings to remain independent of the load currents. Instead, the settings are primarily influenced by the grounding configuration of the power supply.

In medium-voltage solar plants, low-impedance grounding is commonly used, implemented either through a zig-zag transformer (with or without a low-ohmic resistor) or directly via a low-ohmic resistor connected to the transformer neutral. Fig. 2 illustrates the typical connection of a zig-zag transformer in photovoltaic (PV) solar plants, highlighting its interaction with the connected inverters.

Selectivity in ground fault protection is essential to prevent unnecessary tripping of feeders. This can be achieved by:

Grading the time settings of ground fault protection at various system locations.

Applying an inverse time-current curve to minimize the impact of zero-sequence voltage caused by faults in adjacent long cables.

The residual overcurrent feeder protection (50N/51N), connected to the toroidal current transformer, is typically configured to trip at 10–30

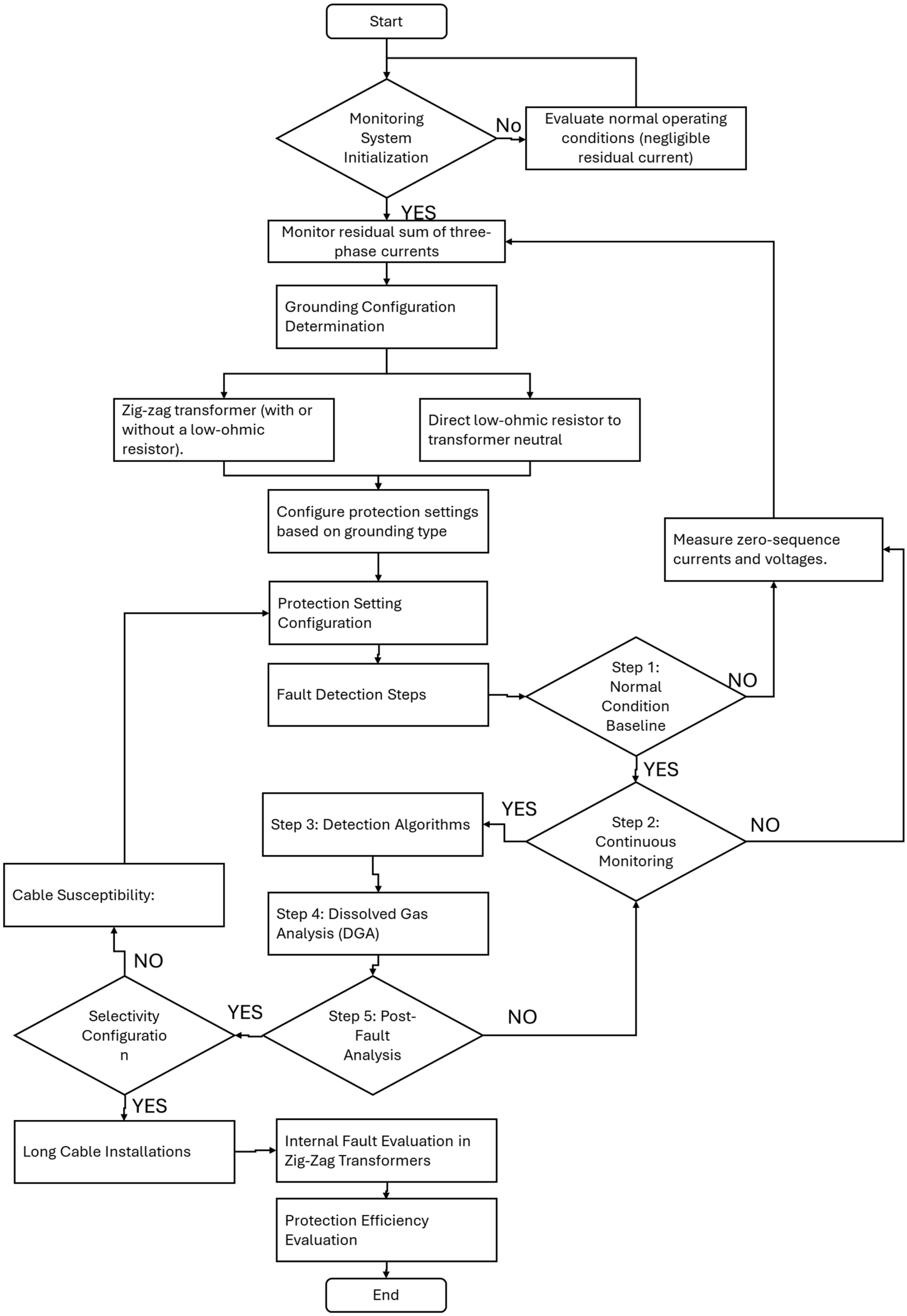

Fig. 1. Methodology for fault detection in zig-zag transformers.

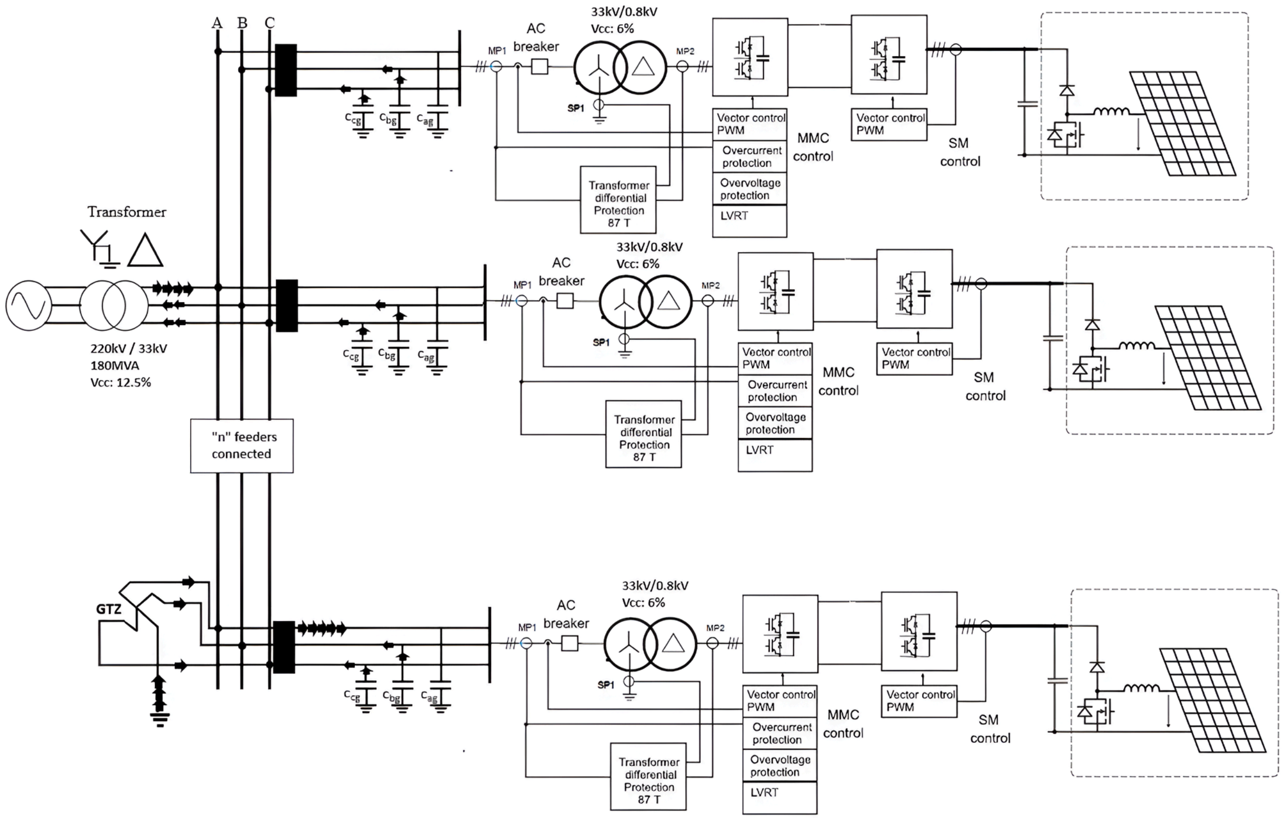

Fig. 2. Connection for the zigzag in PV solar plants with following inverters.

% of the maximum ground fault current. This range is applied uniformly across the entire protection system to ensure consistency

To avoid spurious operations due to variations in current transformers and protection relays, residual overcurrent protection (50N/51N) requires a slight increase in its settings—both in current thresholds and time delays—relative to remote ground overcurrent protection (C-50N/51N).

Additionally, a backup ground fault protection (51 N) can be integrated into the zig-zag transformer. This protection is set above the transformer's continuous thermal capacity current and configured with an extended time delay, typically around 10 s. In systems with very long cable installations, directional neutral overcurrent protection (67 N) is preferred over traditional ground overcurrent protection (50N/51N). This mitigates the risk of unintended tripping caused by residual currents from the earth capacitance of healthy cables.

For faults in the zig-zag transformer, the phase overcurrent function in the feeder relays will directly trip the associated circuit breaker, ensuring fault isolation.

The first threshold for evaluation considers the overload protection of the zig-zag transformer. Under normal conditions, the zig-zag transformer operates with no load, producing only a no-load current. Therefore, the starting point for this protection is set at the lowest value allowed by the relay for an unbalanced linear load, as described by Eq. (1)

$$\begin{bmatrix} I_0 \\ I_1 \\ I_2 \end{bmatrix} = \frac{1}{3} \begin{bmatrix} 0.5 & 0.5 & 0.5 \\ -\alpha^2 & -1 & -\alpha \\ -\alpha & -1 & -\alpha^2 \end{bmatrix} \begin{bmatrix} I_a \\ I_b \\ I_c \end{bmatrix} \tag{1}$$

$$I_N = 3I_0 = 1.5I_{a0} = 0.5I_n \tag{2}$$

- Set the pick-up current at 0.1xIn [5].
- The curve type will be normally inverse with a dial setting of 0.25.
- Inverse Time Curve: IEC Normal Inverse.
- Dial (Time delay): 0.25.
- For short-circuit faults within the zig-zag transformer, the pick-up current is set at 50 % of the fault current at the transformer terminals with a time delay of 100 ms.

About the second threshold to clear short-circuit faults in the zig-zag transformer. Set a pick-up current at 50 % of the fault current at the transformer terminals with a time delay of 100 ms, regarding the Eq. (2) in Eq. (3), with defined time and delay of 0.1s.

$$I_{pickup} = 0.5I_{sc} \tag{3}$$

This methodology ensures that the protection settings are optimized for detecting and isolating ground faults efficiently while maintaining system stability and reliability. Detecting internal faults in a zig-zag transformer requires a robust methodology that considers the unique configuration and operating characteristics of such transformers. The methodology should include continuous monitoring, diagnostic techniques, and protective relays specifically designed to identify anomalies indicative of internal faults.

The steps for the evaluation of internal faults in zig-zag transformers is the following:

- **Step 1:** Normal operating conditions. It establishes a baseline measurement for normal operating currents and voltages in each phase and the neutral point. The Measure and record the zero-sequence currents and voltages under normal operating conditions, as zig-zag transformers typically carry negligible zero-sequence currents unless a fault occurs.

The current transformer connection and overcurrent protection configured with a delta connection on the secondary side, which limits their ability to detect internal imbalances. Effectively, this setup functions akin to having only two overcurrent relays monitoring two phases. During an internal fault within the zig-zag transformer, non-zero currents are detected in these two phases. For instance, in the Fig. 3, a fault was identified in phase B of the zig-zag transformer, triggering overcurrent protections in phases B and C. Specifically, in phase B, a homopolar current was observed, indicating a high-impedance fault (between winding and ground), reaching only 3 %, below the traditional setting of 10 % in the threshold.

Overcurrent protection (50/51) evaluates according to the Fig. 3, to detect excessive current flow, which could indicate short circuits or ground faults; besides, the ground fault protection (50N/51N) evaluates the zero-sequence currents indicative of ground faults.

- **Step 2:** Continuous monitoring and data collection, with accurate current and voltage transformers are installed to provide reliable data to the protective relays and monitoring systems, with oscillography recording for transients and post-event analysis. The methodology was validated using data from 35 zig-zag transformers installed in medium voltage solar plants. Internal inspections were conducted on three of these transformers in a laboratory setting.
- **Step 3:** Detection Algorithms, with differential current analysis with the difference between the primary and secondary currents. Set thresholds for differential current that trigger alarms or trips when exceeded, in Eq. (4).

$$I_{N1} = \frac{1}{25} I_0 = \frac{1}{150} I_n \tag{4}$$

- **Step 4:** Dissolved gas analysis, the evaluation of the hydrogen and methane limits before the fault, on the baseline measurements and expected fault conditions, the evaluation of the maximum values for zig zag transformers is analyzed to improve the diagnostic, as a factor for the Table 2. Concentrations of various gases, including hydrogen, methane, and acetylene, were measured to assess the extent of degradation and potential faults. The DGA results were compared across different operational conditions to identify common failure modes.
- **Step 5:** Post-fault analysis: After a fault is detected, review the oscillographic recordings and relay logs to confirm the fault type and location, to determine the root cause of the fault and implement corrective actions to prevent recurrence, with the trigger alarms for minor faults and trip signals for severe faults regarding the mechanical relays and electrical trip.

Finally, the efficiency of fault detection methods, as follows:

- DGA: Provided an 85.71 % efficiency in predictive recognition of faults without requiring specialized training.
- Comtrade Analysis: Achieved a higher efficiency of 88.57 % but required specialized training.

Table 2
Current international standard for evaluation IEEE [6], for mineral oil.

Elements	Unknown age	1–30 years	Higher 30
Hydrogen (H_2)	80	75	100
Methane (CH_4)	90	45–90	110
Ethane (C_2H_6)	90	30–90	150
Ethylene (C_2H_4)	50	20–50	90
Acetylene (C_2H_2)	1	1	1
Carbon monoxide (CO)	900	900	900
Carbon Dioxide (CO_2)	9000	5000–10,000	10,000

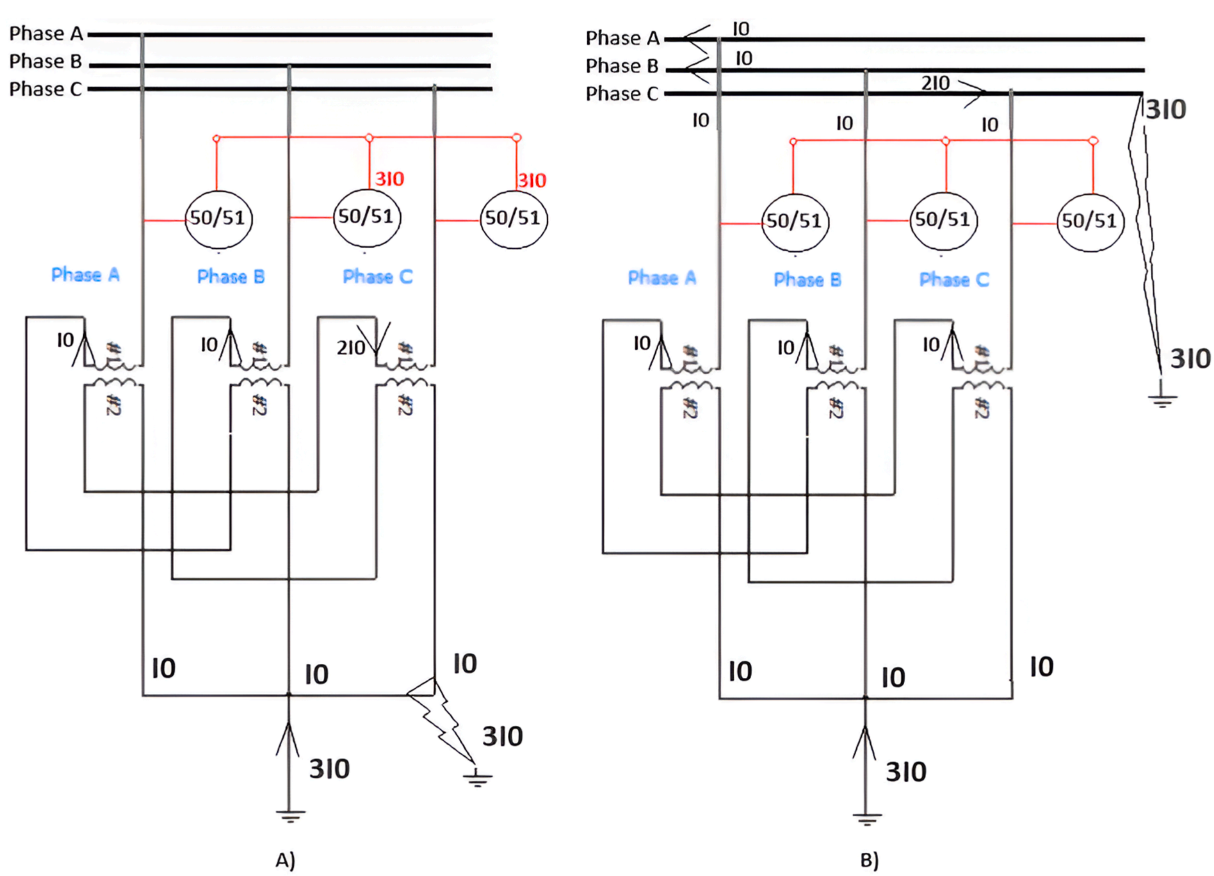

Fig. 3. Case for fault: A) Internal fault. B) External fault.

- Overcurrent Protection: Offered a 45.71 % efficiency but did not provide predictive recognition.
- Differential Protection: Demonstrated a 91.43 % efficiency in fault detection without needing predictive recognition or special training.
- Combined Methodology: The combination of DGA, Comtrade, and overcurrent protection methods improved the overall fault detection efficiency, highlighting the importance of a multi-faceted approach.

2.3. Data

The data for the validation considered 35 zig-zag transformers with application in solar technology in the medium voltage side in delta connection, and the validation of the 3 zig-zag transformers with internal inspection in the laboratory.

In the Table 3, Hydrogen has a mean concentration of 565.37 ppm with a standard deviation of 1538.89 ppm, and values ranging from 0 to 5703 ppm. Methane's mean is 10.23 ppm, with a standard deviation of 19.44 ppm, and ranges from 0 to 70 ppm. Carbon monoxide shows a mean of 145.37 ppm and a standard deviation of 218.44 ppm, with values between 1 and 872 ppm. Carbon dioxide has a mean of 1250.55 ppm and a standard deviation of 2386.11 ppm, ranging from 15 to 9746 ppm. Ethylene's mean is 1.95 ppm, with a standard deviation of 4.89 ppm, and ranges from 0 to 27 ppm. Ethane has a mean of 2.98 ppm, with a standard deviation of 6.31 ppm, and values ranging from 0 to 23 ppm. Acetylene shows a mean of 1.30 ppm and a standard deviation of 4.63 ppm, with values between 0 and 27 ppm. Oxygen's mean is 10,509.69 ppm, with a standard deviation of 7725.45 ppm, and ranges from 849 to 25,843 ppm. Nitrogen has a mean of 37,176.01 ppm and a standard deviation of 21,670.73 ppm, with values between 3218.4 and 101,609 ppm, regarding the Fig. 4.

The validation for the analysis is a laboratory inspection with electrical test to validate the instrument and methodology.

Compared with [11] and [8], and the results in the Fig. 4, it introduces a particular reason about the CO and CO_2 content should not have a significant impact on fault conditions in zig-zag transformers is that their presence is often not directly correlated with fault-specific mechanisms, such as high-energy arcing, overheating of electrical contacts, or partial discharges, which are primary indicators of transformer faults. CO and CO_2 are byproducts of the degradation of cellulose insulation and oil oxidation over time, processes that occur even under normal operating conditions. While their elevated levels can indicate long-term thermal degradation or aging of the transformer, they are not as sensitive to rapid or sudden changes caused by internal faults like stray gassing, arcing, or partial discharge. This limits their utility in detecting early fault conditions or distinguishing between normal aging processes and critical fault scenarios. As a result, CO and CO_2 are considered for the degradation of the insulation (Kraft or paper) as a supplementary indicator for general health monitoring rather than primary fault indicators, but not for zig-zag failure with sudden fault with fast oil degradation.

2.4. Efficiency metrics

In the evaluation of the efficiency, it used the analysis of unbalance database with the evaluation of the Yeo-Johnson transformation, with the evaluation of the positive and non-positive values of the data [11]. Therefore, the transformation function T(y, λ) considered a given data point y and a transformation parameter λ is in the Eq. (5); with $y \geq 0$.

$$T(y,\lambda) = \begin{cases} \left((y+1)^{\lambda} - 1\right)/\lambda, \ \textit{with}\ \lambda \neq 0 \\ \log(y+1), \ \textit{with}\ \lambda = 0 \end{cases} \tag{5}$$

Besides, for the limits: $y < 0$, the Eq. (6).

$$T(y,\lambda) = \begin{cases} \left(-\left(|y|+1\right)^{2-\lambda} - 1\right)\Big/(2-\lambda), \ \textit{with}\ \lambda \neq 2 \\ -\log(|y|+1), \ \textit{with}\ \lambda = 2 \end{cases} \tag{6}$$

With the output process, the gaussian distribution produced a symmetric comparison characterized by its mean (μ) and standard deviation (σ), with the transformed data (;) approximate a normal distribution [11] with the Eq. (7).

$$f(x,\mu,\sigma^2) = \frac{1}{\sqrt{2\pi\sigma^2}} \exp\left(-\frac{(x-\mu)^2}{2\sigma^2}\right) \tag{7}$$

The calculation of the efficiency (η), with the division of the number of correct prediction (CP) between total number of prediction (ToP) in the Eq. (8); and the combination of the number of true positives (TP), number of true negativies, number of false positives (FP), and number of false positives (FN) in the Eq. (9).

$$\eta = \frac{CP}{ToP} \tag{8}$$

$$\eta = \frac{TP + TN}{TP + TN + FP + FN} \tag{9}$$

3. Case study

The case study with 35 zig-zag transformers without the faults with sudden disconnection, however, with failure modes in evolution. The control block for the zig-zag transformer protection with the overcurrent protection for overload and short circuit current in the Fig. 5, besides, the protection of overvoltage and under/protection, on the other hand, the mechanical protection (buchholz, overtemperature, over pressure), it is collected in the zigzag trip contact; and all the signals has a master trip.

The content for normal operation and limits of the operation is the following based on 90th percentile in the Table 4. Therefore, it has the concentration levels of elements in parts per million (ppm) under different operational conditions. It compares the concentrations of Hydrogen (H2), Methane (CH4), Ethane (C2H6), Ethylene (C2H4), Acetylene (C2H2), Carbon Monoxide (CO), and Carbon Dioxide (CO2) for equipment of unknown age, during normal operation, with stray gassing, and at limits before a sudden fault. For instance, Hydrogen levels range from 80 ppm in equipment of unknown age to 5703 ppm before a sudden fault, while Methane remains constant at 250 ppm for normal operation and stray gassing but spikes at 250 ppm before a sudden fault. Ethylene and Carbon Monoxide levels stay unchanged across all conditions, whereas Acetylene increases from 1 ppm in unknown age equipment to 27 ppm before a sudden fault. Carbon Dioxide has the highest concentration, remaining stable at 9000 ppm to 10,000 ppm across all conditions.

Table 3
Description of the database.

Description	hydrogen	methane	carbonMonoxide	carbonDioxide	ethylene	ethane	acetylene	oxygen	nitrogen
Mean	565.4	10.2	145.4	1250.6	1.9	3.0	1.3	10,509.7	37,176.0
Std	1538.9	19.4	218.4	2386.1	4.9	6.3	4.6	7725.4	21,670.7
Min	0.0	0.0	1.0	15.0	0.0	0.0	0.0	849.0	3218.4
25 %	2.0	0.0	15.0	53.0	0.0	0.0	0.0	3888.0	24,091.8
50 %	6.0	1.0	50.0	203.0	1.0	1.0	0.0	7475.0	31,958.5
75 %	22.3	9.5	128.0	679.8	1.0	2.0	1.0	15,558.0	46,332.3
Max	5703.0	70.0	872.0	9746.0	27.0	23.0	27.0	25,843.0	101,609.0

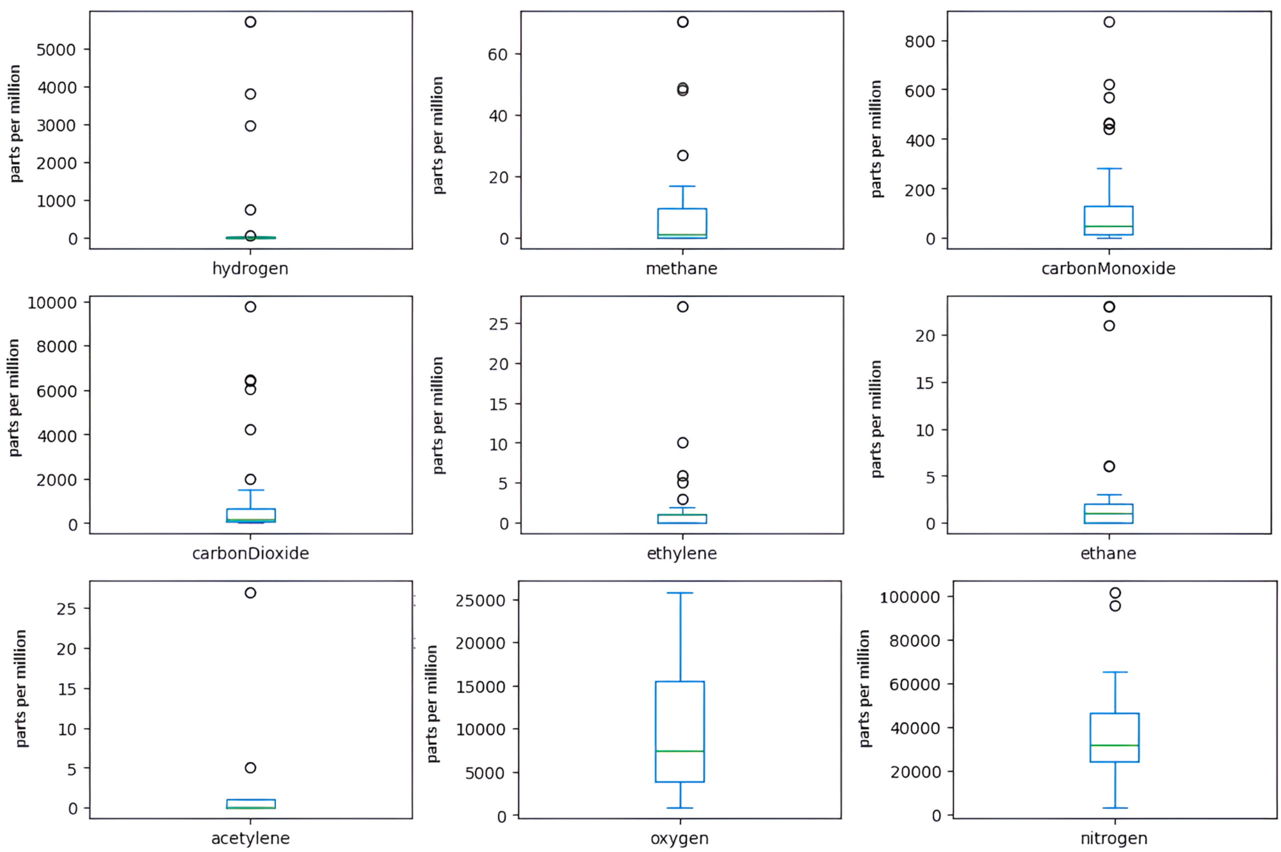

Fig. 4. Box and whiskers plot.

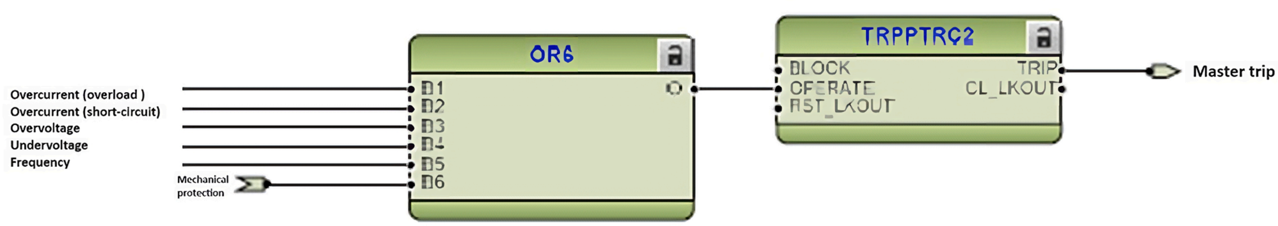

Fig. 5. Mechanical and electrical protection for the trip.

Table 4
Evaluation of the limits in the dissolved gas analysis.

Elements	Unknown age (ppm)	Normal operation (ppm)	Normal with stray gassing (ppm)	Limits before sudden fault (ppm)
Hydrogen (H_2)	80	100	565	5703.0
Methane (CH_4)	90	250	250	250.0
Ethane (C_2H_6)	90	300	350	872.0
Ethylene (C_2H_4)	50	50	50	50.0
Acetylene (C_2H_2)	1	5	5	27.0
Carbon monoxide (CO)	900	1000	1000	1000.0
Carbon Dioxide (CO_2)	9000	10,000	10,000	10,000.0

Therefore, the Table 4 provides data on dissolved gas analysis (DGA) limits, indicating the concentration of specific gases in transformer oil under different operational conditions, the analysis of the conveyed information, particularly regarding CO_2 limits across conditions:

- The CO_2 limits remain constant at 10,000 ppm across all conditions, including "Normal operation," "Normal with stray gassing," and "Limits before sudden fault."
- This suggests that CO_2 levels are less sensitive to fault conditions or stray gassing compared to other gases. It could mean that CO_2 accumulation is typically steady or unrelated to the fault or gassing processes in this scenario.

On the other gases show significant changes, as follows:

- Gases like Hydrogen, Ethan, and Acetylene exhibit significant increases in concentration "before the sudden fault," highlighting their importance as fault indicators.

- For instance, Hydrogen rises dramatically from 565 ppm (stray gassing) to 5703 ppm (sudden fault), signaling a strong correlation with fault occurrence.

It means implications about the interpretation of the CO_2 limits in zig-zag transformer analysis is the following:

- The consistency of CO_2 at 10,000 ppm across all conditions could imply that its levels are not a direct marker of immediate or sudden transformer faults but might indicate long-term thermal degradation.
- In contrast, gases like H_2 and C_2H_2 are critical for identifying rapid changes or faults.

Finally, for the Table 4, the CO_2's stability suggests it is a less dynamic indicator during fault evolution. However, the presence of other elevated gases in conjunction with high CO_2 could provide insights into the fault's nature and progression regarding the kraft degradation.

About the over voltages in solar parks, especially in underground cables, it poses challenges due to their high magnitude and frequency. For instance, in [20] the underground of 5 km cable system with three conversion units, a phase C voltage gap of 95 % was recorded (1 kV), while phases A and C exhibited a voltage rise of 1.73 p.u. (33.1 kV). Under single-phase ground fault conditions, maximum phase currents reached 4.12 kA, with a screen current of 4.56 A at 3.492 kV and a cable current of 85.27 A. Peak transient overvoltage levels of 3.5 p.u. were recorded, threatening cable insulation, and circulating currents contributed over 15 % of the total fault current, exacerbating insulation stress. Surge arresters with tolerances of 10 % for systems below 100 kV and 5 % for higher voltages proved effective in mitigating transient effects with peaks of 1.1 kA against a nominal current of 309 A in inrush current in each energization. Besides, the homopolar current detection enhanced fault identification accuracy by 20 %, while errors in the 630 mm^2 cable cross-section increased from 0.2 % at 1.8 km to 5 % at 5.4 km, highlighting the need for precise system design.

3.1. Internal fault with partial discharge inside the transformer

In the Fig. 6 describes the rebound effect; it is a phenomenon where gas levels, which had previously decreased after the oil treatment, rise again. Therefore, in a first evaluation the stray gassing is an alternative, however, after a new oil replacement and oil impregnate in the kraft solved, it could complicate the interpretation of DGA results and is typically associated with issues like partial discharges. In this case, a partial discharge is detected with a real fault. It evaluates the DGA for mineral oil in a zig-zag transformer, highlighting the concentration of various gases in parts per million (ppm). In untreated oil samples, elevated levels of hydrogen (5703 ppm, 3809.2 ppm, 759 ppm, and 2979 ppm) suggest significant arcing or overheating. Methane, carbon monoxide, and carbon dioxide levels are also higher in untreated samples, indicating insulation degradation and thermal stress. Ethylene, ethane, and acetylene are present in low concentrations, pointing to moderate overheating without extensive arcing. High oxygen and nitrogen levels in untreated samples imply oil degradation and possible air ingress. Conversely, the treated oil sample shows significantly lower gas levels, demonstrating effective treatment in mitigating thermal and electrical stresses within the transformer. The stark contrast in gas concentrations between treated and untreated samples underscores the importance of oil treatment in maintaining transformer reliability and performance. About the five samples:

- Sample 1 (No treatment):
  - Extremely high levels of hydrogen (5703 ppm) suggest significant arcing or severe overheating.
  - Elevated methane (70 ppm), carbon monoxide (55 ppm), and carbon dioxide (604 ppm) levels indicate overheating and some degree of paper insulation degradation.
  - Low levels of ethylene (1 ppm), ethane (23 ppm), and acetylene (1 ppm) suggest moderate overheating without extensive arcing.
  - High Oxygen (19,902 ppm) and nitrogen (43,891 ppm) levels could indicate oil degradation and possible air ingress.
- Sample 2 (No treatment):
  - High hydrogen (3809.2 ppm) indicates significant overheating or arcing.
  - Elevated methane (48.75 ppm), carbon monoxide (32.34 ppm), and carbon dioxide (583.6 ppm) levels confirm overheating and insulation degradation.
  - Low levels of ethylene (1.17 ppm), ethane (21.02 ppm), and acetylene (0.2 ppm) suggest moderate overheating.
  - Oxygen (13,185.8 ppm) and nitrogen (26,274.8 ppm) levels indicate oil degradation and possible air ingress.
- Sample 3 (Treated oil):
  - Very low levels of all gases, including hydrogen (9.2 ppm), methane (0.16 ppm), carbon monoxide (1.02 ppm), and carbon dioxide (23.9 ppm).
  - No ethylene (0 ppm) and very low ethane (0.31 ppm) and acetylene (0 ppm) levels.

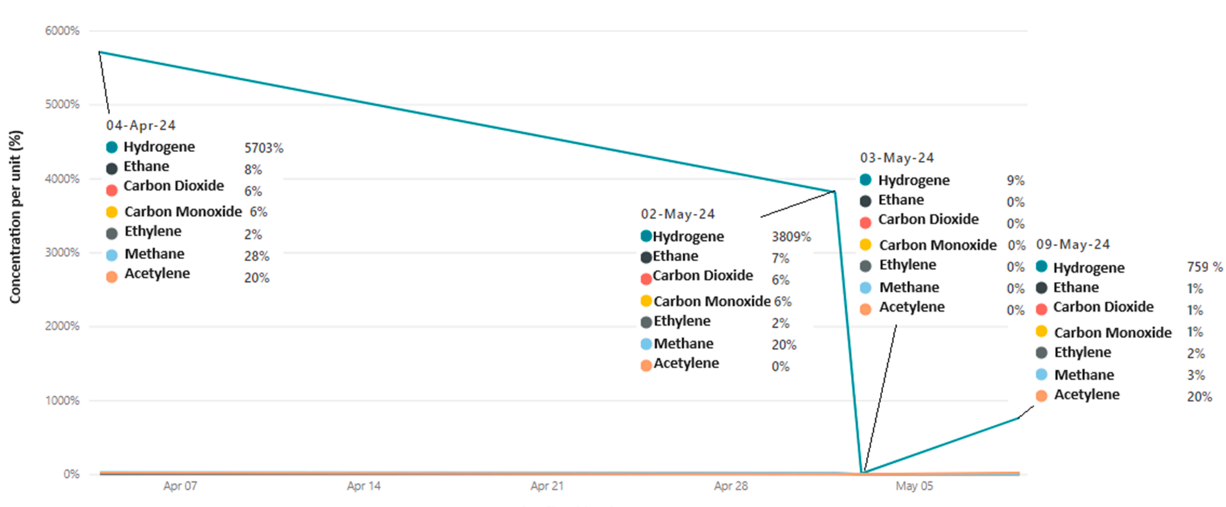

Fig. 6. Case 1 dissolved gas analysis.

  - Significantly lower oxygen (1160.5 ppm) and nitrogen (3218.4 ppm) levels indicate effective treatment, leading to less degradation and reduced presence of gases.
- Sample 4 (No treatment):
  - Moderate hydrogen (759 ppm) levels, indicating minor overheating.
  - Lower levels of methane (7 ppm), carbon monoxide (7 ppm), and carbon dioxide (136 ppm) indicate less severe overheating and minimal insulation degradation.
  - Low ethylene (1 ppm), ethane (2 ppm), and acetylene (1 ppm) levels.
  - Moderate oxygen (3830 ppm) and nitrogen (10,691 ppm) levels suggest some degree of oil degradation and air ingress.
- Sample 5 (No treatment):
  - Elevated hydrogen (2979 ppm) levels indicate significant overheating or arcing.
  - Higher methane (27 ppm), carbon monoxide (17 ppm), and carbon dioxide (240 ppm) levels indicate overheating and some insulation degradation.
  - Low ethylene (1 ppm), ethane (6 ppm), and acetylene (1 ppm) levels.
  - Elevated oxygen (8445 ppm) and nitrogen (25,685 ppm) levels indicate oil degradation and possible air ingress.

In the Reference [16], the transients detected during the faults were in the phases B and C, with currents ranging from 13.8Arms to 15.2Arms in the Fig. 7A), the transformer didnt́ consider a trip due to low short circuit current in the relay. The disconnection was manually without activation of the trip setting. Besides, during the energization of the equipment alone without the busbar 33 kV connected, the peak current of 7.9 Apeak in the phase B, in Fig. 7B); evaluated with the comtrade analysis.

Later, in the Fig. 7C), it detected in phases B and C a fault with values of 19.53A peak and 13.8Arms respectively.

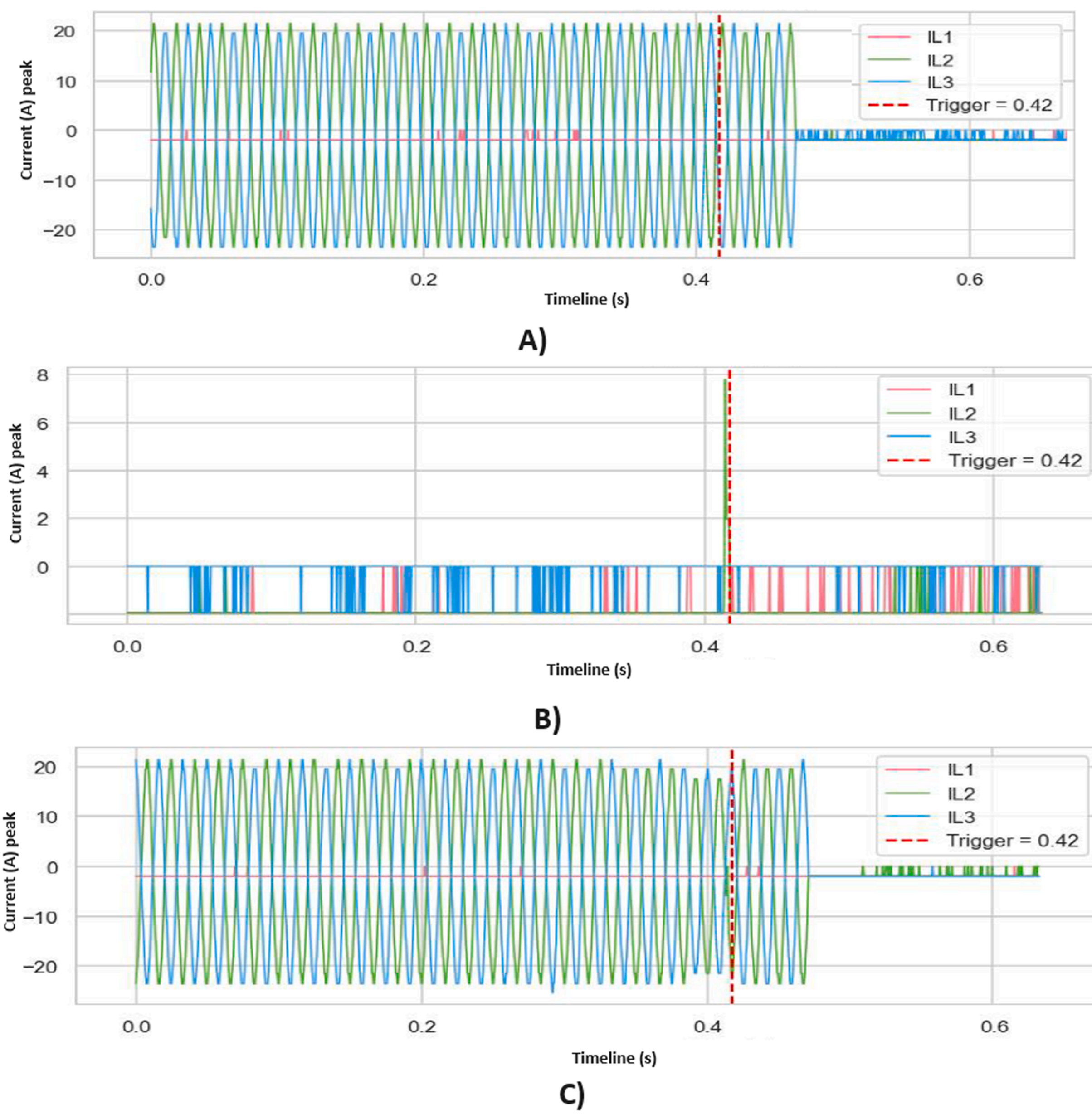

Fig. 7. A) In the beginning of the fault, unbalanced current in the overcurrent protection of the zig-zag transformers. B) Energization process for the evaluation of the fault. C) Energization of the fault with the hot-spot inside the zig-zag transformers [16].

In the rms mode, the values in the phase B and phase C are 15.0Arms and 15.2Arms. In this case, the event is identified by the main transformer differential protection in the Fig. 8. Besides, Fig. 8A) introduced inrush current recorded in the transformer energization, and two additional faults for the underground cable fault and the fault of the current transformer fault due to burden.

In the dissolved gas analysis of the 35 units, the evaluation identified the following common failure modes in evaluation from the Fig. 9 for the statistical modeling, it showed the highly correlated variables could cause multicollinearity, which may distort the interpretation of coefficients in regression models with a threshold higher than 70 % due to case study transformer quantity and the information available according to the recommendation of [8], with an unbalance database with the main characteristics as follows:

- Stray gassing: Hydrogen with higher values of from 100 ppm to 565ppm.
- Partial Discharge: It has two possible defects:
  - Hydrogen required values of 100 ppm to 5703 ppm and Methane with values higher of 250 ppm [7].
  - Hydrogen like the last item, and acetylene from 5 ppm to 27ppm.
- Thermal fault for the oil degradation: Ethylene required values higher of 50 ppm or Ethane with values of 350 ppm to 872ppm. Besides, evolution with hot-spot failures required higher values than 100 ppm in Hydrogen, due to the oil degradation [8].

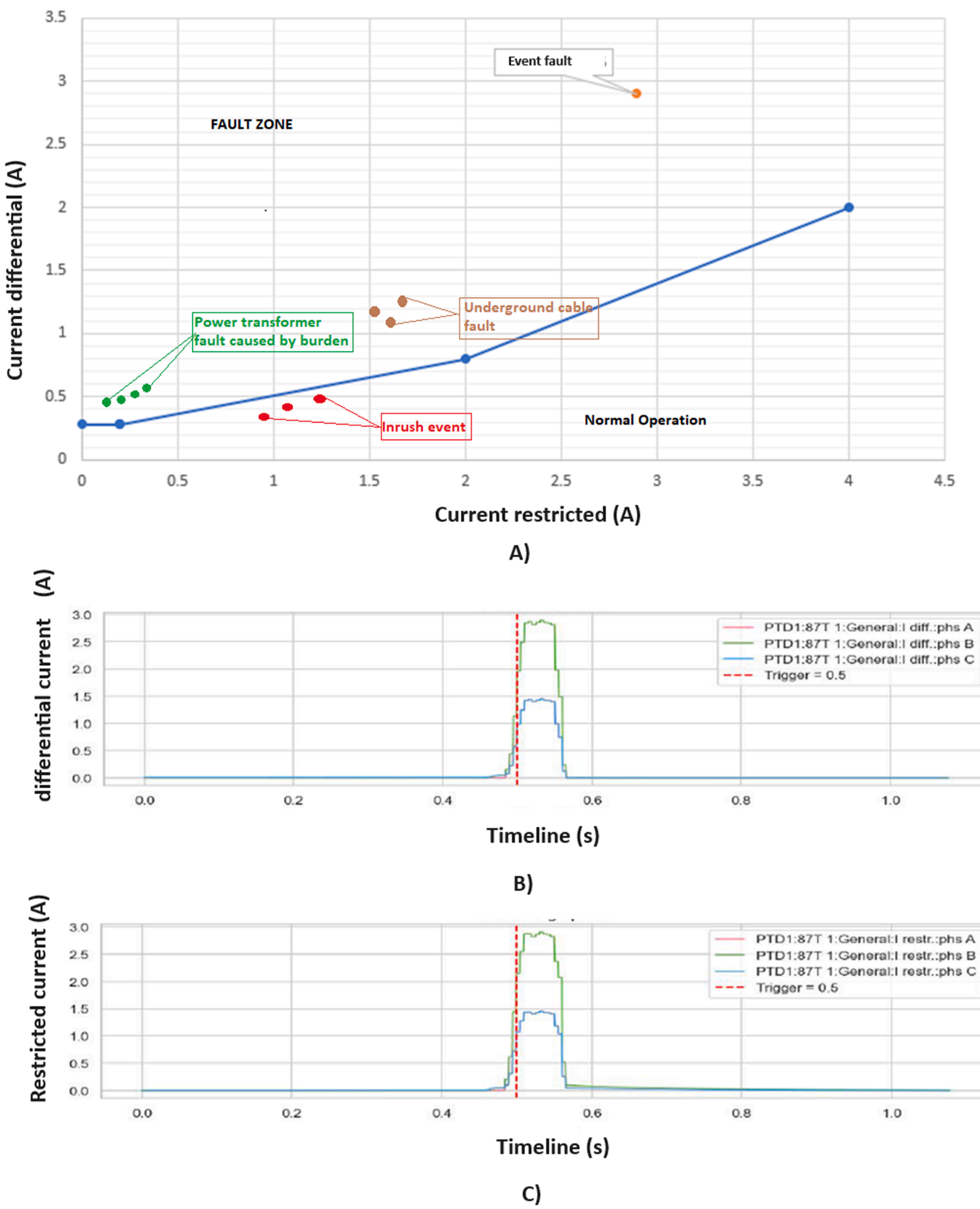

Fig. 8. A) Differential protection zone B) Differential current C) Restricted current.

Fig. 9. Multicollinearity matrix for the dissolved gas analysis in ppm for nine elements.

- Arc faults: It required higher Acetylene values than 5 ppm and Methane with values of 250 ppm. Besides, evolution with hot-spot failures required higher values than 100 ppm in Hydrogen, due to the oil degradation.

About the CO and CO_2 the IEEE Standard proposed limits of CO lower than 1000 ppm and CO_2 lower than 10000 ppm, serves purposes related to transformer health assessment and baseline data calibration, even though these gases may not directly indicate fault conditions, in this case, the presence of CO and CO_2 contributes to understanding the overall condition of the transformer and helps validate other gas readings. For example, unusual increases in CO or CO_2, combined with other fault gases like hydrogen (H_2) or ethylene (C_2H_4), could indicate a potential thermal fault or a hotspot. On the other hand, although CO and CO_2 are not direct fault indicators, their concentrations provide context for interpreting other gases. For instance, an abnormal CO concentration alongside high hydrogen and ethylene levels might point to thermal degradation in conjunction with electrical faults. It means, by monitoring CO and CO_2 within their limits, asset managers can schedule preventive maintenance to address insulation degradation before it escalates into conditions that may trigger faults.

This methodology ensures that the protection settings are optimized for efficient fault detection and isolation while maintaining system stability and reliability. Additionally, the integration of multiple diagnostic tools, including DGA and Comtrade analysis, enhances the accuracy and efficiency of fault detection in zig-zag transformers, contributing to improved overall system performance.

4. Discussion

The evaluation of the case study considered the evaluation on the laboratory; the analysis indicates that the coils experienced an internal short circuit, which destroyed all three windings. It is presumed that the short circuit initiated in phase B, as evidenced by the discharge in the tank and the broken connection cable, caused by electrodynamic stress that ultimately severed the coil connection conductors, it is regarding the partial discharge fault and its evolution in an arc fault. In Fig. 9, the core, consisting of silicon steel laminations, is shown to have shifted, disrupting the arrangement of the sheets.

In Fig. 10, presents a case of an electrical arc fault with sudden acetylene generation. The internal fault was evidenced during an internal inspection, revealing that the coils experienced an internal short circuit, which destroyed all three windings. The short circuit likely originated in phase B, as indicated by evidence of discharge in the tank and a broken connection cable, resulting from electrodynamic forces that ultimately severed the coil connection conductors. The inspection also showed that the silicon steel laminated core had shifted, disrupting the alignment of the sheets, and there was noticeable deformation of the tank's side walls and multiple discharge points.

Electrical arc faults in transformers are severe incidents that can cause extensive damage to the equipment and pose significant safety risks. These faults generate high-energy arcs, leading to the rapid decomposition of insulating materials and the production of gases such as acetylene. The sudden presence of acetylene is a critical indicator of arcing faults and helps in diagnosing the nature and severity of the incident.

In this case, the internal short circuit within the coils resulted in catastrophic damage, destroying the windings and causing phase B to initiate the fault. Electrodynamic forces, which are substantial during short circuits, led to the severing of connection conductors and significant mechanical stress on the transformer's structure. This stress caused the silicon steel laminated core to shift, disrupting its alignment, which can further affect the transformer's magnetic properties and efficiency.

Additionally, the tank's deformation and multiple discharge points indicate that the fault's energy was substantial enough to affect the transformer's physical integrity. Such deformation can compromise the structural strength of the transformer, leading to potential oil leaks and reducing its lifespan.

Preventing such faults involves regular maintenance and monitoring, including dissolved gas analysis (DGA) to detect early signs of gas generation indicative of partial discharges or overheating. Effective cooling and insulation management, along with robust design to withstand electrodynamic forces, are essential for mitigating the risks associated with electrical arc faults in transformers.

Additionally, Fig. 11 shows in the thermal fault with temperature

Fig. 10. Internal laboratory inspection with the fault in the phase B in the zig-zag transformer, for the case study.

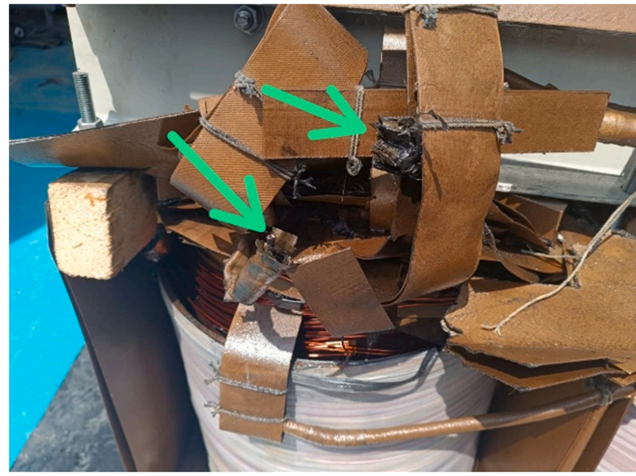

Fig. 11. Thermal fault with hot-spot fault inside the zig-zag transformer.

lower than 250 °C, usually thermal fault T3, that the magnetic body of the upper and lower yokes does not display evident damage.

In the evaluation of the fault, the evolution started in a stray gassing classification and increased the Ethylene for the thermal fault with Duval's triangle, and overheating in the Duval's pentagon.

This effect used the information from the reference [13], it concluded that the temperature gradients in the conductor's circumferential direction are negligible, making a two-dimensional axi-symmetric model sufficient for simulating winding disk temperatures. It was also observed that the temperature measured beneath spacers and in contact with disk walls is lower than the actual conductor temperature, with the difference increasing alongside the heat generation rate and horizontal duct height. For the top disk, this difference can exceed 2 °C; these correlations apply to both-side heating and single-side heating ducts, with Reynolds numbers ranging from 7.5 to 75.9 and 1.5 to 218.4, respectively. The enhanced thermal simulation model aligns well with experimental data on oil and disk temperature distributions. For ducts with both-side heating, Reynolds numbers ranged from 7.5 to 75.9, with a dimensionless distance x* from 0 to 0.01399. For single-side heating, Reynolds numbers ranged from 1.5 to 218.4, with x* ranging from 0 to 0.03484. The accuracy of temperature predictions using the derived correlations was within ±1 °C, showing good agreement with experimental data and supporting the model's use in design calculations and performance predictions for disk-type transformer windings, with heat source of 75 °C with top temperature of 90 °C [14].

Fig. 12. deformation of the tank's side walls and several discharge points.

An additional evidence of the internal fault, Fig. 12 reveals deformation of the tank's side walls and several discharge points, with a partial discharge fault with evolution of the arc fault with temperature higher than 700 °C inside the zig-zag transformers.

Furthermore, Fig. 13 illustrates the fracture of the neutral bushing as a result of the expansion of the zigzag transformer tank with the pressure relief relay action. In the early diagnosis of this post-mortem transformer, it is recommended to rewind the three zigzag cores with enamel-coated aluminum flat wire with class A insulation and to fabricate a new tank, provided the core and magnetic body pass internal insulation tests [9].

In this type of fault, the internal short circuit in the coils could result from several factors, including manufacturing defects, insulation degradation, or operational stresses. The electrodynamic forces during a short circuit could be substantial, causing physical displacement and mechanical damage to the windings and core. The displacement of silicon steel laminations in the core affects the transformer's magnetic properties and can lead to increased losses and overheating. The deformation of the tank and the fracture of the bushing indicate significant internal pressure build-up and mechanical stress, which compromise the transformer's structural integrity. Addressing these faults involves comprehensive diagnostic procedures and thorough inspection to ensure all affected components are identified and properly repaired or replaced to restore the transformer's functionality and reliability.

The Table 5 compares 35 transformers' samples regarding the zigzag transformers fault. About the analysis, highlighting their predictive recognition capabilities, efficiency, and training requirements with a same database of faults. Dissolved Gas Analysis (DGA) effectively predicts potential issues with an efficiency of 85.71 % and requires no specialized training. Comtrade analysis also offers predictive recognition with a higher efficiency of 88.57 % but necessitates specialized training. Overcurrent protection, while not providing predictive recognition, has a lower efficiency of 45.71 % and does not require training. Differential protection is highly efficient at 91.43 % in detecting faults without predictive recognition and does not need special training. A combined methodology of DGA, Comtrade, and overcurrent protection promises enhanced fault detection [10], although its exact efficiency is not provided and requires specialized training. This comparison underscores the importance of choosing the right diagnostic tools based on the specific needs of efficiency and the availability of training resources. Therefore, the improvement was from 88.57 % to 91.43 %, which represents a relative efficiency increase of 3.23 %. This highlights the incremental gains in fault detection efficiency when transitioning from Comtrade analysis to differential protection, in Table 5.

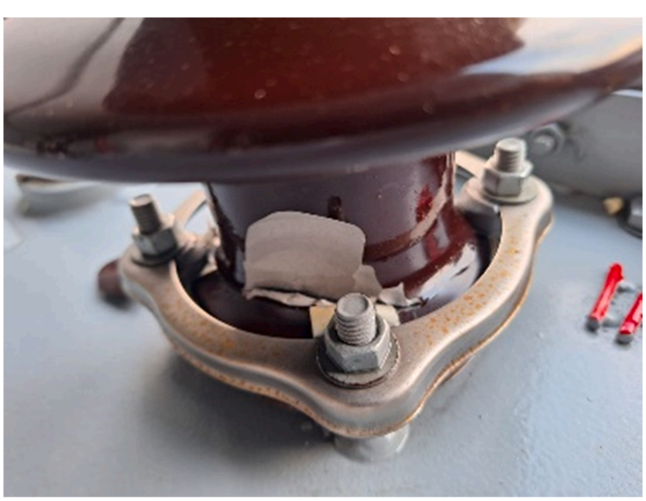

Fig. 13. Laboratory external bushing inspection, the fracture of the neutral bushing as a result of the expansion of the zigzag transformer tank.

Table 5
Efficiency in the fault recognition process.

Methodology	Predictive recognition	Efficiency	Required training
DGA	Yes	85.71 %	No
Comtrade analysis	Yes	88.57 %	Yes
Overcurrent protection [16]	No	45.71 %	No
Differential protection	No	91.43 %	No
DGA + comtrade + overcurrent	Yes		Yes

As a summary, the Table 5 has the following contribution:

- DGA (85.71 %): Effective but slightly less efficient.
- Comtrade Analysis (88.57 %): More efficient than DGA but requires training.
- Differential Protection (91.43 %): The efficient method, offering a marginal improvement (3.23 %) over Comtrade analysis.

Besides, the detection of early faults in flexible transmission systems for instance the DSTATCOM is improved with the Zig-Zag transformer, therefore, without compensation, the source current becomes distorted during unbalanced loads, and the neutral current increases significantly. However, with the DSTATCOM in place, source current distortion is mitigated, and the neutral current is reduced to <10 % of its uncompensated value. Furthermore, the harmonic distortion (THD) in the source current, initially at 51.13 %, is significantly reduced to 5 % with DSTATCOM compensation, while the PCC voltage THD drops from 3.9 % to 1.7 %. In this aspect, the harmonic component increased during the internal fault in the Zig-zag transformer [12].

Finally, the PV solar plants in the tropical zone allows the ambient temperature significantly affects heat transfer within the conversion unit. For instance, an increase in average temperature from 27.6 °C to 31.6 °C results in a 396.24 % increase in heat transfer, while the maximum temperature increases from 44.7 °C to 45.86 °C leads to a 106.27 % rise in heat transfer [15]; >90 °C in the hot spot [14]. This condition increased the overheating problem with delta temperature of 16.27 °C higher than hot spot with 45.86 °C of ambient temperature.

5. Conclusion

The case study on the dissolved gas analysis (DGA) of 35 zig-zag transformers highlights several critical observations and conclusions. Firstly, untreated oil samples displayed significantly elevated levels of hydrogen, methane, carbon monoxide, and carbon dioxide, indicating severe arcing, overheating, and insulation degradation. In contrast, treated oil samples showed a drastic reduction in gas concentrations, emphasizing the effectiveness of oil treatment in mitigating thermal and electrical stresses within transformers. In this research article identified common failure modes such as stray gassing, partial discharges, thermal faults, and arc faults. These modes were characterized by specific gas concentration thresholds, providing valuable diagnostic markers for early fault detection. This research article proposed an improvement for the DGA developed in the IEEE standard [6], for instance, the concentration limits of various gases in parts per million (ppm) for transformers under different operational conditions. For hydrogen (H2), the concentration ranges from 80 ppm in equipment of unknown age to 5703 ppm before a sudden fault. Methane (CH4) remains constant at 250 ppm during normal operation and stray gassing but increases significantly at the fault limit. Ethane (C2H6) levels rise from 90 ppm in unknown age equipment to 872 ppm before a fault. Ethylene (C2H4) remains steady at 50 ppm across all conditions. Acetylene (C2H2) increases from 1 ppm in unknown age equipment to 27 ppm before a fault. Carbon monoxide (CO) stays stable at 1000 ppm during normal and fault conditions.

Carbon dioxide (CO2) shows the highest concentrations, remaining constant between 9000 and 10,000 ppm across all conditions. These gas concentration thresholds are critical for identifying and diagnosing potential transformer faults.

The analysis of transient currents during faults revealed that internal short circuits, primarily initiated in phase B, caused substantial mechanical and thermal stress, leading to severe damage including the deformation of the transformer tank and core misalignment. These findings underscore the critical need for regular monitoring and maintenance, including DGA, to detect and address early signs of faults. Additionally, the study compared various fault diagnosis methodologies, demonstrating the high efficiency of DGA (85.71 %) and Comtrade analysis (88.57 %) in predictive recognition, although Comtrade analysis requires specialized training. Differential protection, while not predictive, showed the highest efficiency (91.43 %) in fault detection without needing special training. This comparison highlights the importance of selecting appropriate diagnostic tools based on efficiency and training requirements. Overall, the study emphasizes the importance of comprehensive diagnostic approaches, combining multiple methodologies to enhance fault detection and transformer reliability. Regular oil treatment and monitoring are crucial for preventing catastrophic failures and maintaining the operational integrity of transformers.

For future works, it should integrate advanced diagnostic tools such as machine learning algorithms and artificial intelligence for predictive maintenance. These technologies could help in early fault detection and more accurate interpretation of DGA results, and improve the design and functionality of transformer protection systems, ensuring they can detect and respond to a wider range of fault conditions, including low-current faults that might not trigger conventional protection mechanisms.

Funding

This paper doesnt receives any funding.

CRediT authorship contribution statement

Ricardo Manuel Arias Velásquez: Writing – review & editing, Writing – original draft, Visualization, Validation, Supervision, Software, Resources, Project administration, Methodology, Investigation, Funding acquisition, Formal analysis, Data curation, Conceptualization. **Renato Fabricio Arias Velásquez:** Writing – review & editing, Writing – original draft, Visualization, Validation, Software, Methodology, Investigation, Formal analysis, Data curation, Conceptualization.

Declaration of competing interest

The authors declare that they have no known competing financial interests or personal relationships that could have appeared to influence the work reported in this paper.

Acknowledgments

Universidad Tecnológica del Perú.

Data availability

Data will be made available on request.

References

[1] N. Dashti, et al., Modelling and analysis of delta-connected power transformers grounded using zig-zag transformer, in: 2022 4th Global Power, Energy and Communication Conference (GPECOM), Nevsehir, Turkey, 2022, pp. 406–413, https://doi.org/10.1109/GPECOM55404.2022.9815643.
[2] O.K. Junior, et al., Evaluation of high impedance faults in delta 13.8 kV distribution network, in: 2021 IEEE PES Innovative Smart Grid Technologies Conference - Latin America (ISGT Latin America), Lima, Peru, 2021, pp. 1–5, https://doi.org/10.1109/ISGTLatinAmerica52371.2021.9543027.
[3] Editor(s) P. Murty, Chapter 9 - substations and neutral grounding, in: P.S.R. Murty (Ed.), Electrical Power Systems, Butterworth-Heinemann, 2017, pp. 183–201, https://doi.org/10.1016/B978-0-08-101124-9.00009-7.
[4] Editor(s) G. Vijayaraghavan, et al., 2 - Grounding of power supply system neutral, in: G. Vijayaraghavan, Mark Brown, Malcolm Barnes (Eds.), Practical Grounding, Bonding, Shielding and Surge Protection, Newnes, 2004, pp. 13–23, https://doi.org/10.1016/B978-075066399-1/50002-2.
[5] G. Kindermann, Proteção de Sistemas Elétricos de Potência, Volume 1, 3. ed., Edição do autor, Florianópolis, 2012.
[6] IEEE, IEEE guide for the interpretation of gases generated in mineral oil-immersed transformers, in: IEEE Std C57.104-2019 (Revision of IEEE Std C57.104-2008), 2019, pp. 1–98, https://doi.org/10.1109/IEEESTD.2019.8890040, 1 Nov.
[7] R. Arias, J. Mejia, Principal components analysis and adaptive decision system based on fuzzy logic for power transformer, Fuzzy Inf. Eng. 9 (4) (2017) 493–514, https://doi.org/10.1016/j.fiae.2017.12.005.
[8] R. Arias, A comprehensive evaluation and advancements in dissolved gas analysis for biodegradable oil in photovoltaic solar plants, Results Eng. 22 (2024) 102314, https://doi.org/10.1016/j.rineng.2024.102314.
[9] A. Tazhibayev, et al., Experimental investigation and evaluation of drying methods for solid insulation in transformers: a comparative analysis, Results Eng. 23 (2024) 102470, https://doi.org/10.1016/j.rineng.2024.102470.
[10] J. Camelo-Daza, et al., Parameter estimation in single-phase transformers via the generalized normal distribution optimizer while considering voltage and current measurements, Results Eng. 21 (2024) 101760, https://doi.org/10.1016/j.rineng.2024.101760.
[11] R. Arias, A comprehensive analysis for wind turbine transformer and its limits in the dissolved gas evaluation, Heliyon 10 (20) (2024) e39449, https://doi.org/10.1016/j.heliyon.2024.e39449.
[12] G. Kumar, C. Babu, A. Zig-Zag, Transformer and three-leg VSC based DSTATCOM for a diesel generator based microgrid, Procedia Technol. 21 (2015) 310–316, https://doi.org/10.1016/j.protcy.2015.10.037.
[13] J. Zhang, et al., Experiments and modeling of heat transfer in oil transformer winding with zigzag cooling ducts, Appl. Therm. Eng. 28 (1) (2008) 36–48, https://doi.org/10.1016/j.applthermaleng.2007.02.012.
[14] Y. Peng, et al., The experimental study of the heat ransfer performance of a zigzag-serpentine microchannel heat sink, Int. J. Therm. Sci. 163 (2021) 106831, https://doi.org/10.1016/j.ijthermalsci.2021.106831.
[15] R. Arias, Thermal influence in the design of DC to AC converters due to climatic change for photovoltaic solar plants, Results Eng. 23 (2024) 102480, https://doi.org/10.1016/j.rineng.2024.102480.
[16] R. Arias, Ensembled methodology for the comtrade analysis regarding medium voltage side in wind park, Results Eng. 23 (2024) 102751, https://doi.org/10.1016/j.rineng.2024.102751.
[17] Editor(s) P. Murty, Chapter 9 - substations and neutral grounding, in: P.S.R. Murty (Ed.), Electrical Power Systems, Butterworth-Heinemann, 2017, pp. 183–201, https://doi.org/10.1016/B978-0-08-101124-9.00009-7.
[18] F. Rong, et al., A novel hybrid arc suppression device for single line-to-ground faults, Int. J. Electr. Power Energy Syst. 153 (2023) 109324, https://doi.org/10.1016/j.ijepes.2023.109324.
[19] Rih-Neng Liao, et al., Modelling and analysis of delta-connected distribution transformers with symmetrical neutral-grounding structure for microgrid networks, Int. J. Electr. Power Energy Syst. 97 (2018) 40–50, https://doi.org/10.1016/j.ijepes.2017.10.014.
[20] R. Arias, Transient analysis of temporary overvoltage and cable faults in underground medium voltage systems, Results Eng. (2024) 103875, https://doi.org/10.1016/j.rineng.2024.103875.